

AD-A145 899

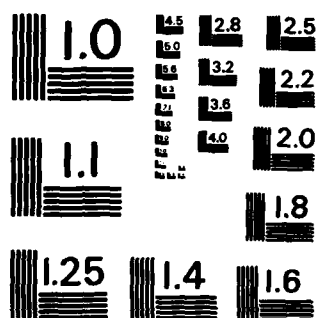
A MATHEMATICAL MODEL OF THE UH-60 HELICOPTER
NATIONAL AERONAUTICS AND SPACE ADMINISTRATION MOFFETT
FIELD CA AMES RESEARCH CENTER K B HILBERT APR 84
NASA-A-9646 NASA-TM-85898 F/G 20/4 NL

UNCLASSIFIED

END

FORMED

DATE



MICROCOPY RESOLUTION TEST CHART
NATIONAL BUREAU OF STANDARDS-1963-A

AD-A145 899

A Mathematical Model of the UH-60 Helicopter

Kathryn B. Hilbert

DTIC FILE COPY

April 1984

DTIC
SELECT
SEP 21 1984
A

This document has been approved
for public release and sale; its
distribution is unlimited.

NASA

National Aeronautics and
Space Administration

United States Army
Aviation Systems
Command



9 09 21 046

A Mathematical Model of the UH-60 Helicopter

Kathryn B. Hilbert, Aeromechanics Laboratory,
U.S. Army Research and Technology Laboratories-AVSCOM
Ames Research Center, Moffett Field, California



National Aeronautics and
Space Administration

Ames Research Center
Moffett Field, California 94035

United States Army
Aviation Systems
Command
St. Louis, Missouri 63120



SYMBOLS

- a blade lift-curve slope, per rad
- a_0 blade coning angle measured from hub plane in the hub-wind axes system, rad
- a_1 longitudinal first-harmonic flapping coefficient measured from the hub plane in the wind-hub axes system, rad
- a_y lateral acceleration, m/sec² (ft/sec²)
- b_1 lateral first-harmonic flapping coefficient measured from hub plane in the wind-hub axes system, rad
- C_T rotor thrust coefficient, $T/\rho(\pi R^2)(\Omega R)^2$
- D Drag force, N (lb)
- H rotor force normal to shaft, positive downwind, N (lb)
- i_{HS} incidence of horizontal stabilator, positive for leading edge up, rad
- K tail rotor cant angle, rad
- K_1 pitch-flap coupling ratio, $\frac{1}{2} \tan \delta_1$
- M fuselage rolling moment, N-m (ft-lb)
- L fuselage lift, N (lb)
- $\left. \begin{matrix} L \\ M \\ N \end{matrix} \right\}$ rolling moment, pitching moment, and yawing moment, respectively, N-m (ft-lb)
- $\left. \begin{matrix} P \\ q \\ r \end{matrix} \right\}$ roll, pitch, and yaw rates in the body-c.g. axes system, rad/sec
- q dynamic pressure, $\frac{1}{2} \rho V^2$, N/m² (lb/ft²)
- Q torque, N-m (ft-lb)
- R rotor radius, m (ft)
- STA longitudinal location in the fuselage axes system, m (ft)
- T thrust, N (lb)

Assignment For	
Wing	Root
Tab	
Location	
Description/	
Availability Codes	
Avail and/or	
Dist	Special
A-1	

- $\left. \begin{matrix} u \\ v \\ w \end{matrix} \right\}$ longitudinal, lateral, and vertical velocities in the body-c.g. system of axes, m/sec (ft/sec)
- v_{iTR} tail rotor induced velocity at rotor disk, m/sec (ft/sec)
- W vertical location in the fuselage axes system, m (ft)
- $\left. \begin{matrix} X \\ Y \\ Z \end{matrix} \right\}$ longitudinal, lateral, and vertical forces in the body-c.g. axes system, N (lb)
- α Stabilizing surface angle of attack, rad
- β rotor sideslip angle, rad
- γ blade lock number, $\rho a c R^2 / I_p$
- δ equivalent rotor blade profile drag coefficient
- δ_a lateral cyclic stick movement, positive to right, cm (in.)
- δ_c collective control input, positive up, cm (in.)
- δ_e longitudinal cyclic stick movement, positive aft, cm (in.)
- δ_p pedal movement, positive right, cm (in.)
- Δ increment in
- θ Euler pitch angle, rad
- θ_o blade root collective pitch, rad
- θ_t total blade twist (root minus tip incidence), rad
- λ inflow ratio, $\lambda = \frac{w_H}{v} = \frac{C_T}{2(u^2 + v^2)^{1/2}}$
- μ rotor advance ratio, $\mu = \frac{\sqrt{u_H^2 + v_H^2}}{\Omega R}$
- ρ air density, kg/m³ (slugs/ft³)
- σ rotor solidity ratio, blade area/disk area
- ϕ Euler roll angle, rad
- ψ Euler yaw angle, rad
- Ω rotor angular velocity, rad/sec

Subscripts:

B body-c.g. axes system relative to air mass
C cant axes system
CV cant-wind axes system
c.g. center of gravity
f fuselage
H hub-body axes system, hub location
HS horizontal stabilator
i induced
p pilot input
TR tail rotor
W hub-wind system of axes

SUMMARY

This report documents the revisions made to a mathematical model of a single main rotor helicopter. These revisions were necessary to model the UH-60 helicopter accurately. The major modifications to the model include fuselage aerodynamic force and moment equations that are specific to the UH-60, a canted tail rotor, a horizontal stabilator with variable incidence, and a pitch bias actuator (PBA). In addition, the model requires a full set of parameters which describe the helicopter configuration and its physical characteristics.

INTRODUCTION

A ten-degree-of-freedom, nonlinear mathematical model that is suitable for real-time piloted simulation of single rotor helicopters is described in reference 1. This simulation model includes the rigid body equations of motion and an aerodynamic model that provide the aerodynamic force and moment characteristics of the aircraft, a generalized stability and control augmentation system, and a simplified engine/governor model.

Revisions to the model were made with the following objectives:

1. Improvement of the fidelity of the UH-60 fuselage aerodynamic model over a wide range of angles of attack and sideslip angles.
2. Modification of the tail rotor aerodynamic model to include the option of canting the tail rotor and modeling its associated aerodynamic effects.
3. Incorporation in the model of the control system for the UH-60 horizontal stabilator with variable incidence and the resultant aerodynamic effects.
4. Incorporation of the UH-60's pitch bias actuator as part of the stability and control augmentation system.

This report describes the four major modifications to the model; the fuselage aerodynamic force and moment equations that are specific to the UH-60, a canted tail rotor, the UH-60 horizontal stabilator with variable incidence, and the UH-60 pitch bias actuator. In addition, a section describing the physical characteristics of the UH-60 and the parameters required by the model is also included.

REVISIONS TO THE FUSELAGE AERODYNAMICS

The UH-60's fuselage aerodynamics were modeled using extensive wind-tunnel test data presented in reference 2. The fuselage force and moment equations were derived from these test data using a regression algorithm (ref. 3). This algorithm basically fits a curve to input data as a nonlinear function of several aerodynamic variables

that are specified by the user (ψ , α , $\sin \psi$, ψ^2 , . . .). These equations replace the fuselage force and moment equations given in reference 1 since they are specific to the UN-60 helicopter.

The equations derived depend on the conventional definition of the angles of attack and sideslip used in the wind tunnel. These angles are not Euler angles. The angle of attack is the geometric angle subtended by the model relative to tunnel axis at zero yaw angle. It is measured relative to the tunnel floor and does not change with yaw angle.

$$\alpha_f \approx \alpha_0 + \tan^{-1} \frac{u_f}{u_0}$$

where

$$u_f \approx u_0 + a_0(\text{STAF} - \text{STAC.G.}) + u_{1f}$$

The sideslip angle is the yaw table angle in the horizontal plane of the tunnel, irrespective of the angle of attack.

$$\beta_f \approx \beta_0 + \tan^{-1} \frac{v_f}{u_f}$$

where

$$v_f \approx v_0 + v_0(\text{STAF} - \text{STAC.G.})$$

The longitudinal forces and moments are dependent on both the angle of attack and on the sideslip angle. The lateral forces and moments are dependent only on the sideslip angle.

Forces:

$$\text{Drag: } \frac{D}{q} = 0.0535 \sin^2 \alpha_f + 41.3404 \cos \alpha_f + 2.96604 \cos \beta_{1f} + 103.161 \cos 2\beta_{1f} + 0.315350 \cdot 10^{-10} \beta_{1f}^2 = 100.2049$$

$$\text{Lift: } \frac{L}{q} = 20.3616 \sin \alpha_f + 33.6480 \sin 2\alpha_f + 41.0424 \sin^2 \alpha_f + 84.3469 \cos \alpha_f + 0.821406 \cdot 10^{-10} \beta_{1f} + 3.07102 \sin \beta_{1f} + 0.0329677 \beta_{1f}^2 = 83.3496$$

$$\text{Sideforce: } \frac{Y}{q} = 33.1440 \sin \beta_{1f} + 21.8010 \sin 2\beta_{1f} + 0.06623 \sin \beta_{1f} + 0.980237 \cdot 10^{-10} \beta_{1f}$$

Moments:

$$\text{Pitching: } \frac{M_x}{q} = 2.37423 \alpha_f + 28.026 \sin 2\alpha_f + 426.760 \sin^2 \alpha_f + 348.072 \cos \alpha_f + 310.301 \cos^2 \beta_{1f} = 36.111$$

$$\text{Rolling: } \frac{M_y}{q} = 614.747 \sin \beta_{1f} + \frac{b^2}{b} (-47.7213 \cos \beta_{1f} + 290.304 \cos^2 \beta_{1f}) + 33.507 \cos^2 \beta_{1f} - 669.766 \quad 25^\circ < \beta_{1f} \leq 90^\circ$$

$$\frac{z}{q} = \frac{v_y}{|v_y|} (455.707 \cos^2 \mu_y - 428.639) \quad 10^\circ < |\mu_y| \leq 25^\circ$$

$$\frac{z}{q} = 0.0 \quad -10^\circ \leq \mu_y \leq 10^\circ$$

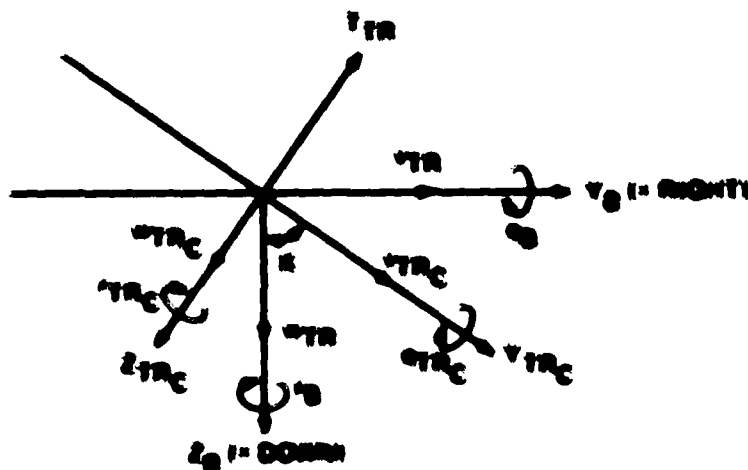
$$\text{Yawing: } \frac{N}{q} = 220.0 \sin 2\mu_y + \frac{v_y}{|v_y|} (671.0 \cos^2 \mu_y - 429.0) \quad 20^\circ < |\mu_y| \leq 90^\circ$$

$$\frac{N}{q} = -278.133 \sin 2\mu_y + 422.644 \sin 4\mu_y - 1.83172 \quad -20^\circ \leq \mu_y \leq 20^\circ$$

Plots of fuselage drag, lift and pitching moment vs the angle of attack are shown in figures 1, 2, and 3. Plots of incremental drag, lift, and pitching moment vs sideslip ($\mu_y = -\mu_x$) are shown in figures 4, 5, and 6. Figures 7, 8, and 9 show fuselage sideforce, rolling and yawing moments vs sideslip. For all these plots, the wind-tunnel data are shown as well as the data generated from the equations derived using the regression algorithm.

CANTED TAIL ROTOR

The UH-60 helicopter was designed with a canted tail rotor mounted on the right side of the vertical fin. In order to find the aerodynamic force and moment contributions from the canted tail rotor it was necessary to introduce two additional axes systems: the cant axis system (subscript C), and the cant-rot axis system (subscript CR). Once these axes systems and the transformations between them have been defined, the development of the tail rotor flapping, force, and moment equations parallel the development done in reference 1 for a noncanted tail rotor (sketch A).



Sketch A

The velocities at the rotor hub in the cant axis system are:

$$v_{TC} = v_{TH}$$

$$v_{TRC} = v_{TH} \cos \mu = v_{TH} \sin \mu$$

$$u_{TRC} = -v_{TR} \cos K + u_{TR} \sin K$$

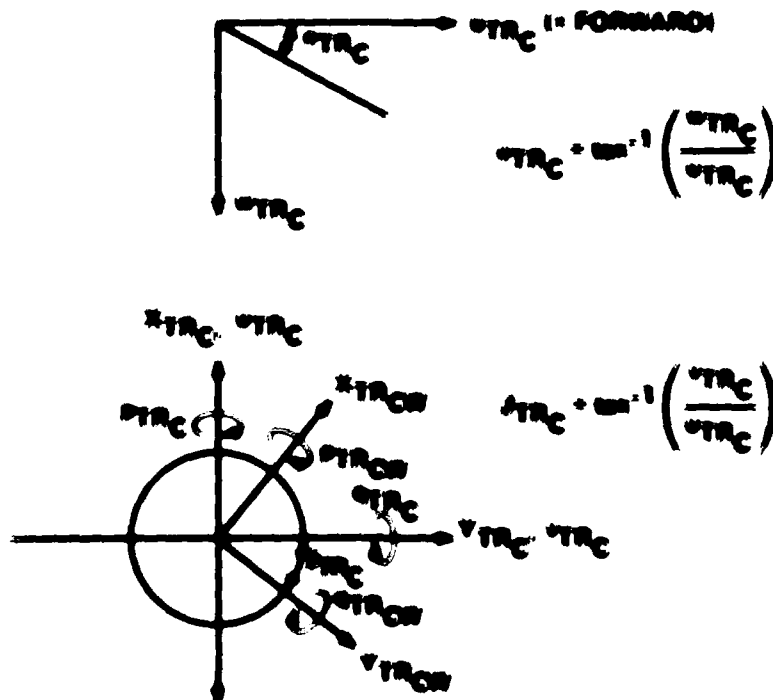
where K = tail rotor cant angle. So when $K = 0^\circ$, the cant axis system coincides with the axis system codirectional with the body-c.g. system.

$$v_{TRC} = u_{TR} \quad u_{TRC} = -v_{TR}$$

The advance ratio for the tail rotor in the cant axis system is:

$$J_{TRC} = \frac{\sqrt{u_{TRC}^2 + v_{TRC}^2}}{R_{TR} \Omega_{TR}}$$

The angles of attack and sideslip for the tail rotor in the cant axis system are defined as (Sketch B):



Sketch B

The angular velocities in the cant axis system are:

$$p_{TRC} = p_B$$

$$q_{TRC} = r_B \cos K + q_B \sin K$$

$$r_{TRC} = -q_B \cos K + r_B \sin K$$

The roll and pitch rates in the cant-wind axis system are:

$$P_{TC_{CW}} = q_{TC} \sin \delta_{TC} + P_{TC} \cos \delta_{TC}$$

$$q_{TC_{CW}} = -P_{TC} \sin \delta_{TC} + q_{TC} \cos \delta_{TC}$$

The flapping coefficients are:

$$a_{TC} = \frac{1}{1 - TC_C} \left[k_{1TC} \left(1 + \frac{1}{2} TC_C \right) f_{1TC} - \left(1 + \frac{1}{2} TC_C \right) f_{2TC} \right]$$

$$b_{TC} = \frac{1}{1 - TC_C} \left[\left(1 - \frac{1}{2} TC_C \right) f_{1TC} + k_{1TC} \left(1 + \frac{1}{2} TC_C \right) f_{2TC} \right]$$

where:

$$TC_C = 1 - \frac{TC_C}{4} = k_{1TC} \left(1 + \frac{1}{2} TC_C \right) \left(1 + \frac{1}{2} TC_C \right)$$

$$f_{1TC} = \frac{1}{2} TC_C^2 a_{TC} = \frac{10}{1 - TC} P_{TC_{CW}} = \frac{q_{TC_{CW}}}{TC}$$

$$f_{2TC} = \frac{8}{3} k_{1TC} TC_C^2 a_{TC} = \frac{16 q_{TC_{CW}}}{1 - TC} = TC_C \left(\frac{8}{3} TC_C + 2 C_{TC} + 2 TC \right) = \frac{P_{TC_{CW}}}{TC}$$

The forces on the tail rotor in the cant-wind axis system ($P_{TC_{CW}}$, $q_{TC_{CW}}$, $V_{TC_{CW}}$, $\delta_{TC_{CW}}$) are the same as the equations given in reference 1 with r_{TB} , P_{TB} , q_{TB} , δ_{TB} , b_{TB} , and v_{TB} replaced by $P_{TC_{CW}}$, $q_{TC_{CW}}$, $V_{TC_{CW}}$, $\delta_{TC_{CW}}$, $b_{TC_{CW}}$, and $v_{TC_{CW}}$, respectively, where the rotor blade profile drag coefficient is:

$$C_{TC} = 0.009 + 0.1 \left(\frac{C_{T_{TC_{CW}}}}{TC_{TC}} \right)$$

and the inflow ratio is:

$$v_{TC} = \frac{q_{TC_{CW}}}{TC_{TC}} = \frac{C_{T_{TC_{CW}}}}{2 \sqrt{1 - TC_C} + TC_{TC}}$$

The induced velocity at the tail rotor is:

$$v_{i_{TRC}} = -\lambda_{TR} R_{TR} \Omega_{TR} + u_{TRC}$$

$$v_{i_{TR}} = -v_{i_{TRC}} \cos K$$

The forces on the tail rotor in the cant axis system can be calculated using a transformation from cant-wind axes to cant axes:

$$X_{TRC} = -R_{TRCW} \cos A_{TRC} - Y_{TRCW} \sin A_{TRC}$$

$$Y_{TRC} = Y_{TRCW} \cos A_{TRC} - X_{TRCW} \sin A_{TRC}$$

$$Z_{TRC} = -Z_{TRCW}$$

Similarly, through another transformation, the body axis forces and moments can be calculated:

$$X_{TR} = X_{TRC}$$

$$Y_{TR} = -Z_{TRC} \cos K + Y_{TRC} \sin K$$

$$Z_{TR} = Y_{TRC} \cos K + Z_{TRC} \sin K$$

$$M_{TR} = -Q_{TRCW} \cos K + Z_{TR} (STA_{TR} - STA_{C.G.}) - X_{TR} (WL_{TR} - WL_{C.G.})$$

$$L_{TR} = Y_{TR} (WL_{TR} - WL_{C.G.})$$

$$N_{TR} = Q_{TRCW} \sin K - Y_{TR} (STA_{TR} - STA_{C.G.})$$

HORIZONTAL STABILATOR

The purpose of a horizontal stabilator with variable incidence is to eliminate excessively nose-high attitudes at low airspeed caused by downwash impingement on the stabilator and to optimize pitch attitudes for climb, cruise, and accelerational descent.

The position of the horizontal stabilator for the UH-60 is programmed between 0.0° trailing-edge-up and 39.0° trailing-edge-down as a function of four variables:

1. Airspeed
2. Collective Control Position
3. Pitch Rate
4. Lateral Acceleration

A detailed description of each of these four feedback loops is given in reference 2.

Figure 10 is a block diagram of the UH-60 horizontal stabilator control system (ref. 2). This logic has been incorporated in the generalized stability and control augmentation system of the math model. The stabilator logic also includes the provision for a fixed horizontal tail incidence that is to be specified by the pilot.

PITCH BIAS ACTUATOR

The UH-60's control system includes a pitch bias actuator (PBA), a variable length control rod which changes the relationship between longitudinal cyclic control and swashplate tilt as a function of three flight parameters: pitch attitude, pitch rate, and airspeed. The main purpose of the PBA is to improve the apparent static longitudinal stability of the aircraft. A detailed description of the PBA is given in reference 2.

The PBA was modeled directly from the block diagram shown in figure 11 (ref. 2). The airspeed feedback is only active between 80 and 180 knots since below 80 knots, the airspeed feedback for the stabilator performs the same stability function. The pitch attitude and rate feedback is active throughout the entire speed range. As can be seen from the block diagram, the PBA actuator authority is 15% of longitudinal cyclic full throw and has a maximum rate limit on the actuator travel of 3% per sec. The output of the PBA is added to the total longitudinal cyclic control. The PBA logic includes an on/off switch to inactivate the PBA, if desired.

UH-60 DESCRIPTION REQUIREMENTS

Table 1 lists the parameters required to model the UH-60 and the values used in the math model. This table is identical to table J-1 in reference 1, except that most of the required fuselage parameters have been eliminated because of the modifications to the fuselage aerodynamic model. The values listed for the UH-60 in table 1 were obtained from reference 2.

Table 2 lists the nonzero feedforward, crossfeed, and feedback gains for the UH-60 control system (see fig. 4 of ref. 1). A detailed description of the four control couplings is given in reference 2.

Table 3 lists the parameters that are required to model the two General Electric T700-GE-700 engines that power the UH-60 and the values that are used in the math model. These values are based on available T700-GE-700 engine data for the AH-64 helicopter.

UH-60 TRIM CHARACTERISTICS

Table 4 lists the four control positions, δ_e , δ_a , δ_c , and δ_p , the lateral and vertical velocities in body axes, v_y and w_b , and the Euler pitch and roll angles, θ and ϕ , for the UH-60 trimmed in level flight at a variety of airspeeds.

UH-60 STABILITY DERIVATIVES

Stability derivatives for the UH-60 math model are presented in Table 1. These derivatives were generated under the following conditions:

- level flight
- pitch bias actuator on
- horizontal stabilator active
- engine/governor model off

Stability perturbation sizes:

$\Delta r_B = 5.0 \text{ deg/sec}$	$\Delta r_B = 5.0 \text{ deg/sec}$
$\Delta \delta_e = 0.1 \text{ in.}$	$\Delta \delta_e = 0.1 \text{ in.}$
$\Delta \delta_a = 0.1 \text{ in.}$	$\Delta \delta_a = 0.1 \text{ in.}$
$\Delta \delta_c = 0.1 \text{ in.}$	$\Delta \delta_c = 0.1 \text{ in.}$
$\Delta \delta_p = 0.1 \text{ in.}$	$\Delta \delta_p = 0.1 \text{ in.}$

Longitudinal stability derivatives were obtained by considering positive and negative perturbations about a reference trim condition. The resulting derivatives are as follows:

$$\begin{aligned} M_{\dot{\alpha}} &= \frac{1}{I_{yy}} \frac{\partial M}{\partial \dot{\alpha}} \\ L_{\dot{\alpha}} &= \frac{1}{I_{xx}} \frac{\partial L}{\partial \dot{\alpha}} \\ N_{\dot{\alpha}} &= \frac{1}{I_{zz}} \frac{\partial N}{\partial \dot{\alpha}} \end{aligned}$$

MODEL VALIDATION

Validation of the UH-60 math model was accomplished by comparison of trim and stability derivatives that were generated from the UH-60 math model with data that were generated from a detailed total force and moment math model of the UH-60, developed by the Advanced Digital/Optical Control System (ADOCS) program.

Tables 1 through 10 show level flight trim characteristics and dimensional stability derivatives generated by the Boeing-Vertol UH-60 math model for comparison with data generated in tables 4 through 10. These derivatives were generated under the same conditions as the UH-60 derivatives were, but with significantly larger aircraft gross weight, and a faster main rotor.

rotational velocity. Figures 12 through 17 illustrate six of the more important UH-60 stability derivatives vs airspeed. For these plots, the UH-60 data are shown as well as the data generated from the Boeing-Vertol UH-60 math model.

CONCLUDING REMARKS

The mathematical model of a UH-60 helicopter described in this report was developed for real-time piloted simulation. To date, this model has been used successfully in two handling qualities simulation experiments on the six-degree-of-freedom Vertical Motion Simulator (VMS) at NASA Ames Research Center (refs. 5 and 6) in support of the ADOCS program.

For these simulations, however, high levels of stability augmentation were added to the baseline UH-60 math model, thus effectively masking many of the characteristics of the basic aircraft. The baseline UH-60 model has not been evaluated in real-time piloted simulations nor has it been validated with flight data to determine the accuracy with which it models the actual aircraft dynamics and handling qualities. In addition, neither the analog and digital stability augmentation system (SAS) nor the flight path stabilization (FPS) system of the actual UH-60 helicopter is included in the model.

REFERENCES

1. Talbot, P. D.; Tinling, B. E.; Decker, W. A.; and Chen, R. T. N.: A Mathematical Model of a Single Main Rotor Helicopter for Piloted Simulation. NASA TM-84281, September 1982.
2. Howlett, J. J.: UH-60A Black Hawk Engineering Simulation Program, Volumes I and II. NASA CR-166309 and CR-166310, December 1981.
3. Systems Control, Inc.: SCI Model Structure Determination Program (OSR) User's Guide. NASA CR-159084, November 1979.
4. Landis, K. H.; and Aiken, E. W.: An Assessment of Various Side-Stick Controller/ Stability and Control Augmentation Systems for Night Nap-of-the-Earth Flight Using Piloted Simulation. Helicopter Handling Qualities. NASA CP-2219, April 1982.
5. Landis, K. H.; Dunford, P. J.; Aiken, E. W.; and Hilbert, K. B.: A Piloted Simulator Investigation of Side-Stick Controller/Stability and Control Augmentation System Requirements for Helicopter Visual Flight Tasks. AHS Paper A-83-39-59-4000, May 1983.
6. Landis, K. H.; Glusman, S. I.; Aiken, E. W.; and Hilbert, K. B.: An Investigation of Side-Stick Controller/Stability and Control Augmentation System Requirements for Helicopter Terrain Flight Under Reduced Visibility Conditions. AIAA Paper 84-0235, January 1984.

TABLE 1.- UH-60 DESCRIPTION REQUIREMENTS

Description	Algebraic symbol	Computer mnemonic	Units	UH-60
<u>Main rotor (MR) group</u>				
MR rotor radius	R_{MR}	ROTOR	ft	26.83
MR chord	c_{MR}	CHORD	ft	1.73
MR rotational speed	Ω_{MR}	OMEGA	rad/sec	27.0
Number of blades	n_b	BLADES	N-D	4.0
MR Lock number	γ_{MR}	GAMMA	N-D	8.1936
MR hinge offset	ϵ	EPSLN	percent/100	.04659
MR flapping spring constant	K_β	AKBETA	lb-ft/rad	0
MR pitch-flap coupling tangent of δ_3	K_1	AKONE	N-D	0
MR blade twist	θ_{tMR}	THETT	rad	-.3142
MR precone angle (required for teetering rotor)	a_{0MR}	AOP	rad	0
MR solidity	σ_{MR}	SIGMA	N-D	.08210
MR lift curve slope	a_{MR}	ASLOPE	rad ⁻¹	5.73
MR maximum thrust	C_{Tmax}	CTM	N-D	.1846
MR longitudinal shaft tilt (positive forward)	i_s	CIS	rad	.05236
MR hub stationline	STA_H	STAH	in.	341.2
MR hub waterline	WL_H	WLH	in.	315.0
<u>Tail rotor (TR) group</u>				
TR radius	R_{TR}	RTR	ft	5.5
TR rotational speed	Ω_{TR}	OMTR	rad/sec	124.62
TR Lock number	γ_{TR}	GAMATR	N-D	3.3783
TR solidity	σ_{TR}	STR	N-D	.1875
TR pitch-flap coupling tangent of δ_3	K_{1TR}	FKITR	N-D	.7002
TR precone	a_{0TR}	AOTR	rad	.01309
TR blade twist	θ_{tTR}	THETR	rad	-.3142
TR lift curve slope	a_{TR}	ATR	rad ⁻¹	5.73
TR hub stationline	STA_{TR}	STATR	in.	732.0
TR hub waterline	WL_{TR}	WLTR	in.	324.7

TABLE 1.- CONTINUED

Description	Algebraic symbol	Computer mnemonic	Units	UH-60
<u>Aircraft mass and inertia</u>				
Aircraft weight	W_{ic}	WAITIC	lb	16400.0
Aircraft roll inertia	I_{XX}	XIXXIC	slug-ft ²	5629.0
Aircraft pitch inertia	I_{YY}	XIYYIC	slug-ft ²	40000.0
Aircraft yaw inertia	I_{ZZ}	XIZZIC	slug-ft ²	37200.0
Aircraft cross product of inertia	I_{YZ}	XIXZIC	slug-ft ²	1670.0
Center of gravity stationline	$STA_{c.g.}$	STACG	in.	360.4
Center of gravity waterline	$WL_{c.g.}$	WLCCG	in.	247.2
Center of gravity butto line	$BL_{c.g.}$	BLCCG	in.	0
<u>Fuselage (Fus)</u>				
Fus aerodynamic reference point stationline	STA_{ACF}	STAACF	in.	345.5
Fus aerodynamic reference point waterline	WL_{ACF}	WLACF	in.	234.0
<u>Horizontal stabilizer (HS)</u>				
HS station	STA_{HS}	STAHS	in.	700.4
HS waterline	WL_{HS}	WLHS	in.	244.0
HS incidence angle	i_{HS}	AIHS	rad	variable
HS area	S_{HS}	SHS	ft ²	45.0
HS aspect ratio	AR_{HS}	ARHS	N-D	4.6
HS maximum lift curve slope	$C_{L_{maxHS}}$	CLMHS	N-D	1.03
HS dynamic pressure ratio	η_{HS}	XNH	N-D	.4
Main rotor induced velocity effect at HS	K_{VMR}	XXVMR	N-D	1.8
<u>Vertical fin (VF)</u>				
VF stationline	STA_{VF}	STAVF	in.	695.0
VF waterline	WL_{VF}	WLVF	in.	273.0
VF incidence angle	i_{VF}	AIFF	rad	0
VF area	S_{VF}	SF	ft ²	32.3
VF aspect ratio	AR_{VF}	ARF	N-D	1.92
VF sweep angle	Λ_F	ALMF	rad	.7156
VF maximum lift curve slope	$C_{L_{maxVF}}$	CLMF	N-D	.89
VF dynamic pressure ratio	η_{VF}	VNF	N-D	.651
Tail rotor induced velocity effect at VF	k_{VTR}	XXVTR	N-D	1.0

TABLE 1.- CONCLUDED

Description	Algebraic symbol	Computer mnemonic	Units	UM-60
<u>Controls</u>				
Swashplate lateral cyclic pitch for zero lateral cyclic stick	C_{A1S}	CA1S	rad	0
Swashplate longitudinal cyclic pitch for zero longitudinal cyclic stick	C_{B1S}	CB1S	rad	0
Longitudinal cyclic control sensitivity	CK_1	CK1	rad/in.	.04939
Lateral cyclic control sensitivity	CK_2	CK2	rad/in.	.02792
Main rotor root collective pitch for zero collective stick	C_5	C5	rad	.2286
Main rotor collective control sensitivity	C_6	C6	rad/in.	.02792
Tail rotor root collective pitch for zero pedal position	C_7	C7	rad	.1743
Pedal sensitivity	C_8	C8	rad/in.	-.07734

TABLE 2.- UH-60 CONTROL SYSTEM CHARACTERISTICS

Description	Algebraic symbol	Computer mnemonic	UH-60
<u>Feedforward gains</u>			
Longitudinal stick to longitudinal cyclic	t_o/t_{op}	SK(1)	1.0
Lateral stick to lateral cyclic	t_a/t_{ap}	SK(5)	1.0
Collective stick to collective control	t_c/t_{cp}	SK(9)	1.0
Pedals to directional control	t_p/t_{pp}	SK(10)	1.0
<u>Crossfeed gains</u>			
Collective stick to longitudinal cyclic	t_o/t_{cp}	SK(4)	-.1640
Pedals to longitudinal cyclic	t_o/t_{pp}	SKM(2)	-.5746
Collective stick to lateral cyclic	t_a/t_{cp}	SK(8)	-.16
Collective stick to directional control	t_p/t_{cp}	SK(11)	-.7009
<u>Feedback gains</u>			
Pitch rate to lateral cyclic	t_o/q_b	SKV(3,2)	1.3
Roll rate to longitudinal cyclic	t_o/p_b	SKV(6,1)	-.08

TABLE 3.- UH-60 ENGINE CHARACTERISTICS

Description	Algebraic symbol	Computer mnemonic	Units	UH-60 T700-GE-700
<u>Engine/governor</u>				
Engine gain	K_E	NPK	HP/LB _{fuel}	1.75
Engine time constant	τ_E	NPT	sec	1.25
Throttle time constant	τ_t	TWTAC	sec	1.25
Throttle position		TWROT	°	100.0
NR rpm lower limit	ω_{LIN}	ONLIN	rad/sec	9.0
Gear ratio	ω_{TR}/ω_{NR}	TRGEAR	B-D	4.62
Proportional governor feedback gain	K_{B_1}	GRG1	LB _{fuel} /rad/sec	2000.0
Integral governor feedback gain	K_{B_2}	GRG2	LB _{fuel} /rad/sec	2500.0
Rate governor feedback gain	K_{B_3}	GRG3	LB _{fuel} /rad/sec	500.0

TABLE 4.- LEVEL FLIGHT TRIM CHARACTERISTICS

Engineering symbol	Equivalent airspeed, knots						units
	1.0	20.0	40.0	60.0	100.0	160.0	
ξ	0.1266	-0.3670	-0.7083	-0.4738	-1.063	-1.800	in.
ξ_A	.2321	-.9956	-.7560	-.2322	.1812	.3066	in.
ξ_C	5.719	5.361	4.580	4.196	4.425	5.718	in.
ξ_P	-1.279	-1.066	-.5830	-.5802	-.7606	-.005715	in.
η_B	-.006069	-.00037	-.00960	9.989	7.996	8.813	ft/sec
η_D	.1685	3.430	5.108	6.133	7.264	-1.235	ft/sec
δ	5.052	5.834	4.360	3.489	2.669	-.2996	deg
δ	-2.360	-1.362	-1.005	0	0	0	deg

TABLE 5. - X-FORCE STABILITY MODIFICATIONS

Engineering symbol	Equivalent stress, ksi							Units
	1.0	20.0	40.0	60.0	80.0	100.0	120.0	
X_u	-0.02369	-0.01040	-0.01122	-0.01000	-0.01230	-0.01230	-0.01000	1/sec
X_v	-0.03402	-0.02237	-0.00814	-0.02750	-0.005930	-0.02750	-0.02750	1/sec
X_w	0.02542	0.03743	0.04705	0.0414	0.0477	0.0477	0.0400	1/sec
X_q	2.800	2.020	3.221	3.352	3.700	3.700	3.670	ft/sec
X_p	-2.505	-1.100	-0.3700	-0.1303	-1.132	-1.132	-1.304	ft/sec
X_r	-2.071	-1.151	-0.1700	-0.0001	-0.0055	-0.0055	-0.0001	ft/sec
X_{uq}	-1.650	-1.502	-1.400	-1.402	-1.003	-1.003	-1.700	ft/sec
X_{vq}	0.4150	0.1200	0.1003	0.1002	-0.1050	-0.1050	0.0000	ft/sec
X_{wq}	0.700	0.707	0.004	0.011	0.461	0.461	0.144	ft/sec
X_{pq}	0.944	0.143	0.036	0.005	0.000	0.000	0.070	ft/sec

TABLE 6. - 3-AXIS STABILITY DERIVATIVES

Engineering symbol	Equivalent aligned, knots								Units
	1.0	20.0	40.0	60.0	80.0	100.0	140.0		
Z_u	0.02276	-0.1460	-0.1252	-0.06761	-0.00053	-0.0003375	1/sec		
Z_w	-0.000074	-0.02567	-0.01531	-0.02012	-0.01720	-0.01757	1/sec		
Z_p	-0.2931	-0.3036	-0.5017	-0.6006	-0.7007	-0.8006	1/sec		
Z_q	0.004	2.277	2.005	3.502	4.001	0.020	ft/sec/sec		
Z_r	-0.01077	0.002	0.002	1.350	2.076	3.025	ft/sec/sec		
Z_s	-0.2050	-0.3000	-0.4176	-0.6001	-0.5056	-0.3500	ft/sec/sec		
$Z_{\dot{u}}$	-0.1372	-1.077	-2.070	-3.271	-0.120	-0.110	ft/sec./sec.		
$Z_{\dot{w}}$	0.00162	0.05133	0.00053	0.3733	0.5077	0.077	ft/sec./sec.		
$Z_{\dot{p}}$	-1.021	-1.377	-1.470	-0.326	-0.620	-10.76	ft/sec./sec.		
$Z_{\dot{q}}$	0.301	1.076	1.076	2.372	3.005	3.505	ft/sec./sec.		

TABLE 1. - 1960-1961 WINTER SURVEY

Station	Number of birds observed						Total number of birds
	0-1	2-3	4-5	6-7	8-9	10-11	
1	100	100	100	100	100	100	600
2	100	100	100	100	100	100	600
3	100	100	100	100	100	100	600
4	100	100	100	100	100	100	600
5	100	100	100	100	100	100	600
6	100	100	100	100	100	100	600
7	100	100	100	100	100	100	600
8	100	100	100	100	100	100	600
9	100	100	100	100	100	100	600
10	100	100	100	100	100	100	600
11	100	100	100	100	100	100	600
12	100	100	100	100	100	100	600
13	100	100	100	100	100	100	600
14	100	100	100	100	100	100	600
15	100	100	100	100	100	100	600
16	100	100	100	100	100	100	600
17	100	100	100	100	100	100	600
18	100	100	100	100	100	100	600
19	100	100	100	100	100	100	600
20	100	100	100	100	100	100	600
21	100	100	100	100	100	100	600
22	100	100	100	100	100	100	600
23	100	100	100	100	100	100	600
24	100	100	100	100	100	100	600
25	100	100	100	100	100	100	600
26	100	100	100	100	100	100	600
27	100	100	100	100	100	100	600
28	100	100	100	100	100	100	600
29	100	100	100	100	100	100	600
30	100	100	100	100	100	100	600
31	100	100	100	100	100	100	600
32	100	100	100	100	100	100	600
33	100	100	100	100	100	100	600
34	100	100	100	100	100	100	600
35	100	100	100	100	100	100	600
36	100	100	100	100	100	100	600
37	100	100	100	100	100	100	600
38	100	100	100	100	100	100	600
39	100	100	100	100	100	100	600
40	100	100	100	100	100	100	600
41	100	100	100	100	100	100	600
42	100	100	100	100	100	100	600
43	100	100	100	100	100	100	600
44	100	100	100	100	100	100	600
45	100	100	100	100	100	100	600
46	100	100	100	100	100	100	600
47	100	100	100	100	100	100	600
48	100	100	100	100	100	100	600
49	100	100	100	100	100	100	600
50	100	100	100	100	100	100	600

TABLE 8.- MOMENT STABILITY DERIVATIVES

Engineering symbol	Equivalent assumed, knots							Unit
	1.0	20.0	40.0	60.0	80.0	100.0	140.0	
$M_{\dot{\theta}}$	0.007154	0.001005	-0.0002137	0.001079	0.007507	0.005550	rad/sec	
$M_{\dot{\psi}}$	0.01350	0.01115	0.007026	0.006016	0.01630	0.007079	rad/sec	
$M_{\dot{\phi}}$	0.002026	0.003613	0.006760	0.000916	0.00217	0.00023	rad/sec	
$M_{\dot{\theta}\dot{\psi}}$	-0.0161	-0.0010	-0.0001	-0.00230	-0.0001	-0.0001	1/sec	
$M_{\dot{\psi}\dot{\phi}}$	0.1130	0.2006	0.2660	0.2000	0.1031	0.007000	1/sec	
$M_{\dot{\phi}\dot{\theta}}$	-0.001152	-0.000076	-0.00066	-0.00130	-0.0039	-0.0061	1/sec	
$M_{\dot{\theta}\dot{\phi}}$	0.1360	0.1516	0.1721	0.1907	0.1506	0.1230	rad/sec	
$M_{\dot{\psi}\dot{\theta}}$	-0.001159	-0.000026	-0.001697	0.001201	0.00279	0.00490	rad/sec	
$M_{\dot{\phi}\dot{\psi}}$	0.001137	0.00730	0.00350	0.00025	0.00007	0.00007	rad/sec	
$M_{\dot{\theta}\dot{\phi}\dot{\psi}}$	0.01530	-0.000390	-0.00009	-0.00330	-0.00330	-0.00330	rad/sec	

TABLE 6. - LONGITUDINAL STABILITY DERIVATIVES

Derivative symbol	Equations developed. Units							Units
	1.0	20.0	40.0	60.0	80.0	100.0	140.0	
$L_{\dot{u}}$	0.07627	0.02327	-0.003702	-0.000222	-0.000139	0.001010	0.001010	rad/sec/sec
$L_{\dot{w}}$	-0.06124	-0.01956	-0.00663	-0.00000	-0.00000	-0.00000	-0.00000	rad/sec/sec
$L_{\dot{p}}$	0.005022	0.01340	0.02030	0.02500	0.02500	0.02500	0.02500	rad/sec/sec
$L_{\dot{q}}$	-2.272	-1.230	-1.566	-1.522	-1.522	-1.522	-1.522	1/sec
$L_{\dot{r}}$	-3.551	-3.606	-3.010	-3.056	-3.011	-3.011	-3.011	1/sec
$L_{\dot{p}p}$	0.07667	0.04470	0.0220	0.0175	0.0150	0.0150	0.0150	1/sec
$L_{\dot{p}q}$	0.06303	0.04024	0.0100	0.0100	0.0100	0.0100	0.0100	rad/sec./sec.
$L_{\dot{p}r}$	1.336	1.130	1.329	1.310	1.310	1.310	1.310	rad/sec./sec.
$L_{\dot{q}p}$	-1.671	-0.00000	0.00000	0.00000	0.00000	0.00000	0.00000	rad/sec./sec.
$L_{\dot{q}r}$	-0.0000	-1.230	-1.000	-0.016	-1.163	-1.163	-1.163	rad/sec./sec.

TABLE 10.- M-MOMENT STABILITY DERIVATIVES

Engineering symbol	Equivalent airspeed, knots						Units
	1.0	20.0	40.0	60.0	100.0	140.0	
N_u	0.002149	-0.005618	-0.005796	-0.003739	-0.002896	-0.003813	rad/ft/sec
N_v	.009759	.008366	.01245	.01529	.01823	.01979	rad/ft/sec
N_w	-.001943	-.003705	-.006419	-.01079	-.01253	-.007266	rad/ft/sec
N_q	-.3396	-.7563	-.5837	-.4874	-.4424	-.5254	1/sec
N_p	-.1013	-.2857	-.2310	-.1499	-.1136	-.1801	1/sec
N_r	-.3342	-.3662	-.5336	-.6547	-.8515	-1.011	1/sec
$M_{\delta e}$.001120	-.009063	-.01760	-.03105	-.04719	.005004	rad/in./sec ²
$M_{\delta a}$.02734	.02695	.02598	.02691	.02582	.02299	rad/in./sec ²
$M_{\delta c}$.06306	.06005	.01613	-.04757	-.1096	-.08942	rad/in./sec ²
$M_{\delta p}$.6040	.5550	.5701	.6785	.8460	.9274	rad/in./sec ²

TABLE 11 - LEVEL FLIGHT TRIM CHARACTERISTICS
BOEING-VERVOL UH-60 MATH MODEL

Variable	Equivalent airspeed, knots					Units
	20.0	40.0	60.0	100.0	140.0	
L 1947	0.5938	0.3636	0.5149	-0.5356	-1.0539	in.
L 1948	-0.7920	-0.7106	-0.3199	-0.1098	-0.0917	in.
L 1949	5.0054	4.2440	3.8582	4.2054	5.6883	in.
L 1950	-0.2409	-0.05631	-0.1254	.0974	.1798	in.
L 1951	0	0	13.165	9.4517	11.308	ft/sec
L 1952	4.0507	6.5824	3.8820	4.8946	-13.840	ft/sec
L 1953	6.9262	5.5167	2.2425	1.6799	-3.3533	deg
L 1954	-1.6093	-1.2929	0	0	0	deg

TABLE 12 - X, Y, AND Z-FORCE STABILITY DERIVATIVES
BOEING-VERVOL UH-60 MATH MODEL

Variable	Equivalent airspeed, knots					Units
	20.0	40.0	60.0	100.0	140.0	
X 1955	0.0184	-0.0274	-0.0201	-0.0422	-0.0517	1/sec
X 1956	-1.5711	-1.3039	-1.2532	-0.7256	-0.2927	ft/in./sec ²
X 1957	-0.0523	-0.0693	-0.0950	-0.1336	-0.1749	1/sec
X 1958	0.9417	.9417	.9148	.9364	.9924	ft/in./sec ²
X 1959	-1.6223	-1.6140	-1.7968	-2.1322	-2.3677	ft/in./sec ²
X 1960	-0.1332	-0.1332	-0.0546	-0.0158	-0.0324	1/sec
X 1961	-0.3475	-0.5395	-0.6523	-0.7658	-0.8418	1/sec
X 1962	-1.0026	-1.8678	-3.0911	-5.8800	-8.8178	ft/in./sec ²
X 1963	-0.1266	-7.8250	-9.0061	-10.4761	-11.8225	ft/in./sec ²
X 1964	1.1830	1.7228	2.5612	4.3935	6.3606	ft/in./sec ²

TABLE 13.- M-MOMENT STABILITY DERIVATIVES
BOEING-VERTOL UH-60 MATH MODEL

Engineering symbol	Equivalent airspeed, knots						Units
	0.5	20.0	40.0	60.0	100.0	140.0	
M_u	0.0005	0.0091	-0.0043	0.0040	0.0022	0.0019	rad/ft/sec
M_v	.0085	.0022	-.0006	.0011	-.0019	-.0068	rad/ft/sec
M_w	.0021	.0122	.0050	.0072	.0082	.0113	rad/ft/sec
M_q	-.7674	-1.0262	-1.2832	-1.5541	-1.9808	-2.1616	1/sec
M_p	.2938	.2859	.2567	.2379	.1797	.1937	1/sec
M_r	-.0688	-.0595	-.1181	-.1149	-.0860	-.0750	1/sec
M_{δ_e}	.3287	.3366	.3850	.4133	.4543	.4997	rad/in./sec ²
M_{δ_a}	-.0051	.0042	.0134	.0128	.0397	.0585	rad/in./sec ²
M_{δ_c}	-.0183	-.0352	.1574	.1362	.1294	.1418	rad/in./sec ²
M_{δ_p}	.0411	-.0010	-.0499	-.0562	-.0881	-.1113	rad/in./sec ²

TABLE 14.- L-MOMENT STABILITY DERIVATIVES
BOEING-VERTOL UH-60 MATH MODEL

Engineering symbol	Equivalent airspeed, knots						Units
	0.5	20.0	40.0	60.0	100.0	140.0	
L_v	-0.0260	-0.0250	-0.0267	-0.0258	-0.0304	-0.0343	rad/ft/sec
L_q	-1.7256	-1.8067	-1.5485	-1.4919	-1.3987	-1.4051	1/sec
L_p	-3.3484	-3.5455	-3.7116	-3.7659	-3.6853	-3.3574	1/sec
L_r	.2119	.3507	.4149	.4878	.6814	.8556	1/sec
L_{δ_a}	1.3118	1.3297	1.3147	1.2866	1.2907	1.3128	rad/in./sec ²
L_{δ_p}	-.9313	-.8816	-.8968	-1.0035	-1.1990	-1.3063	rad/in./sec ²

TABLE 15.- N-MOMENT STABILITY DERIVATIVES
BOEING-VERTOL UH-60 MATH MODEL

Engineering symbol	Equivalent airspeed, knots						Units
	0.5	20.0	40.0	60.0	100.0	140.0	
N_v	0.0081	0.0108	0.0119	0.0141	0.0176	0.0195	rad/ft/sec
N_p	-.1856	.0322	.0251	-.0446	-.0706	-.0955	1/sec
N_r	-.2879	-.3902	-.5142	-.6283	-.8389	-1.0394	1/sec
N_{δ_a}	.0266	-.0286	-.0268	-.0110	.0014	.0032	rad/in./sec ²
N_{δ_c}	.0665	.0576	.0222	-.0191	-.0544	-.0041	rad/in./sec ²
N_{δ_p}	.7153	.6731	.6720	.7668	.9319	1.0023	rad/in./sec ²

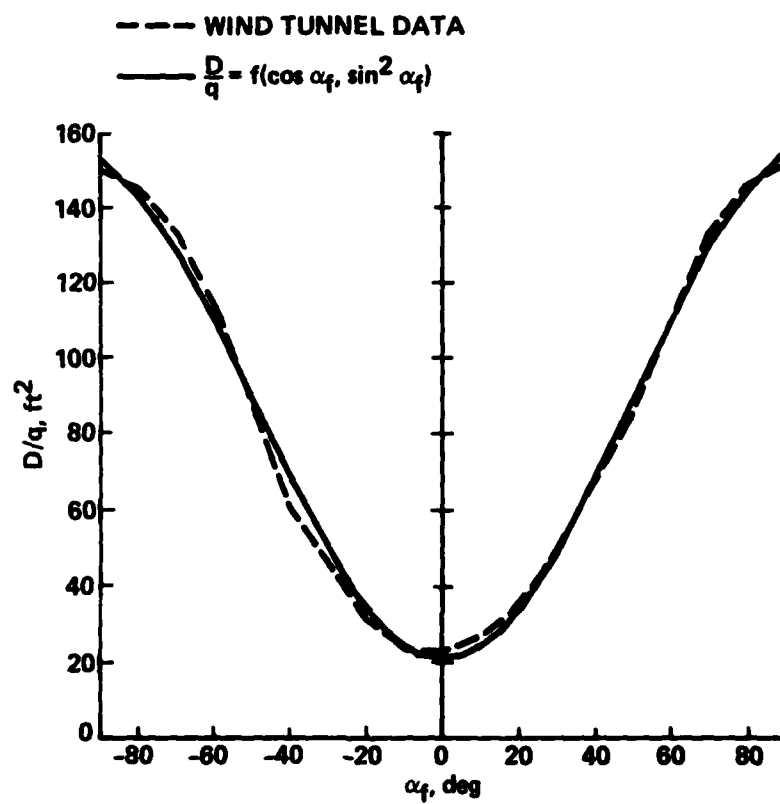


Figure 1.- Fuselage drag vs angle of attack.

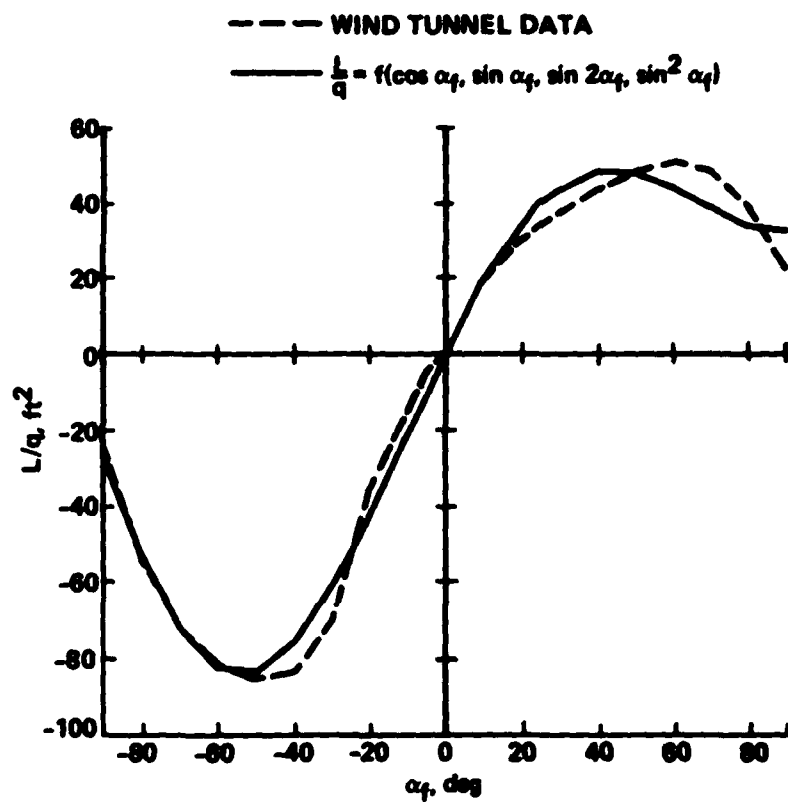


Figure 2.- Fuselage lift vs angle of attack.

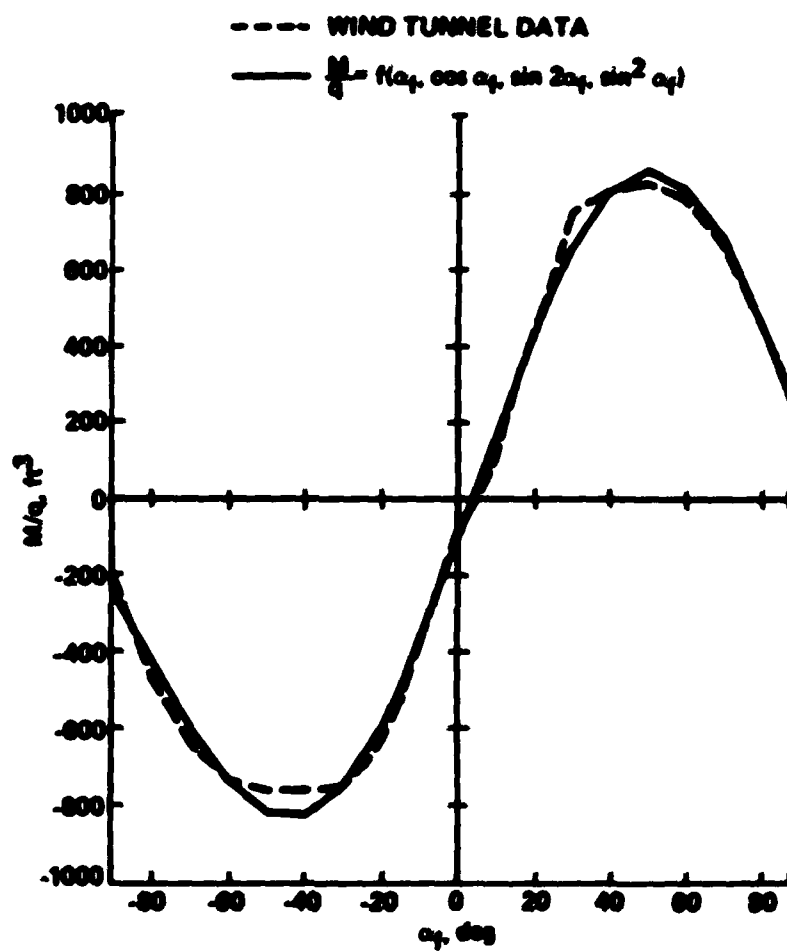


Figure 3.- Fuselage pitching moment vs angle of attack.

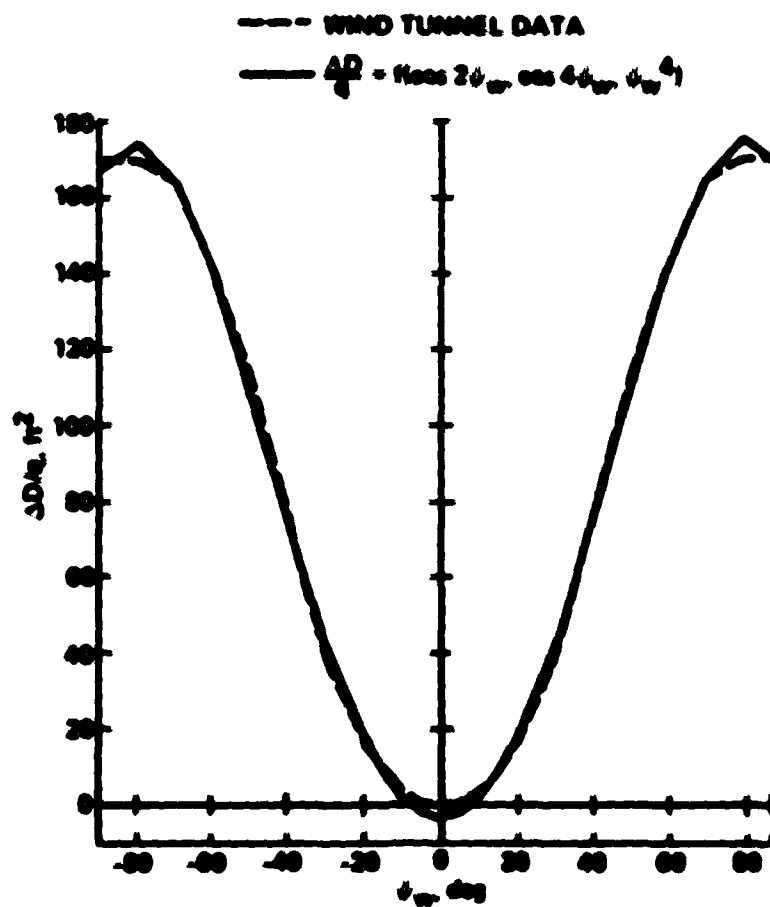


Figure 4.- incremental fuselage drag vs sideslip.

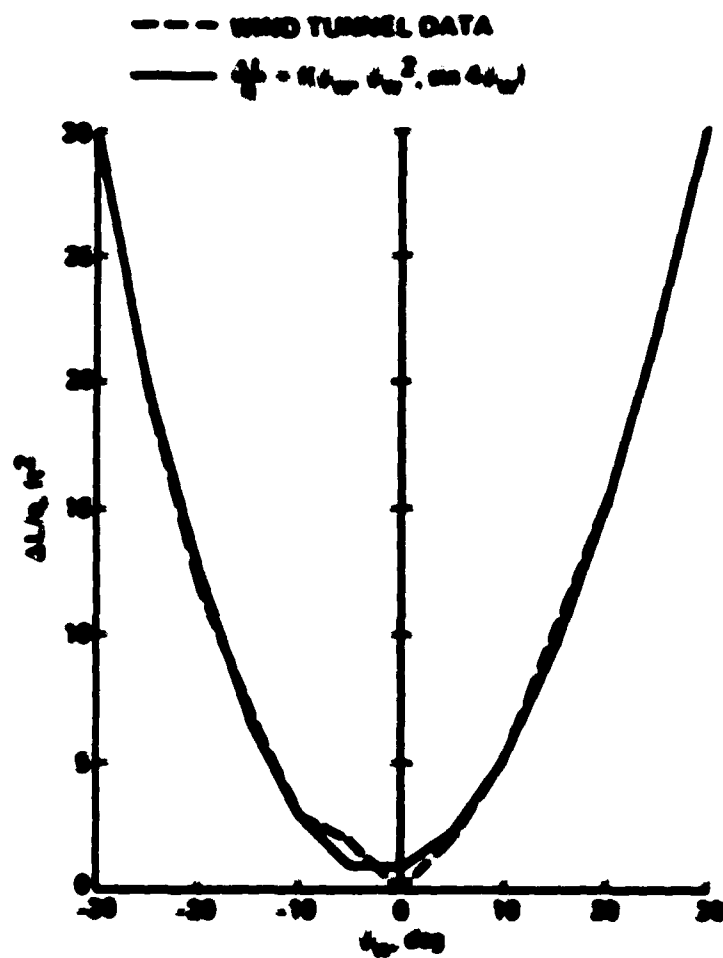


Figure 5.- Incremental fuselage lift vs sideslip.

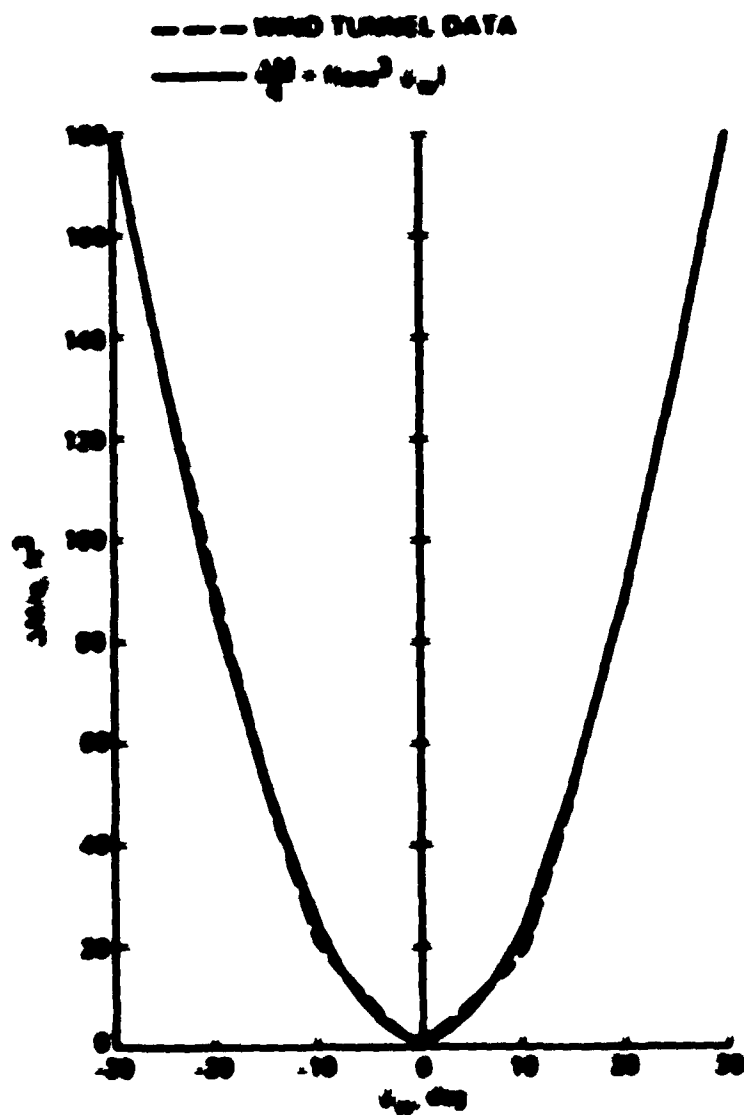


Figure 6.- Incremental fuselage pitching moment vs sideslip.

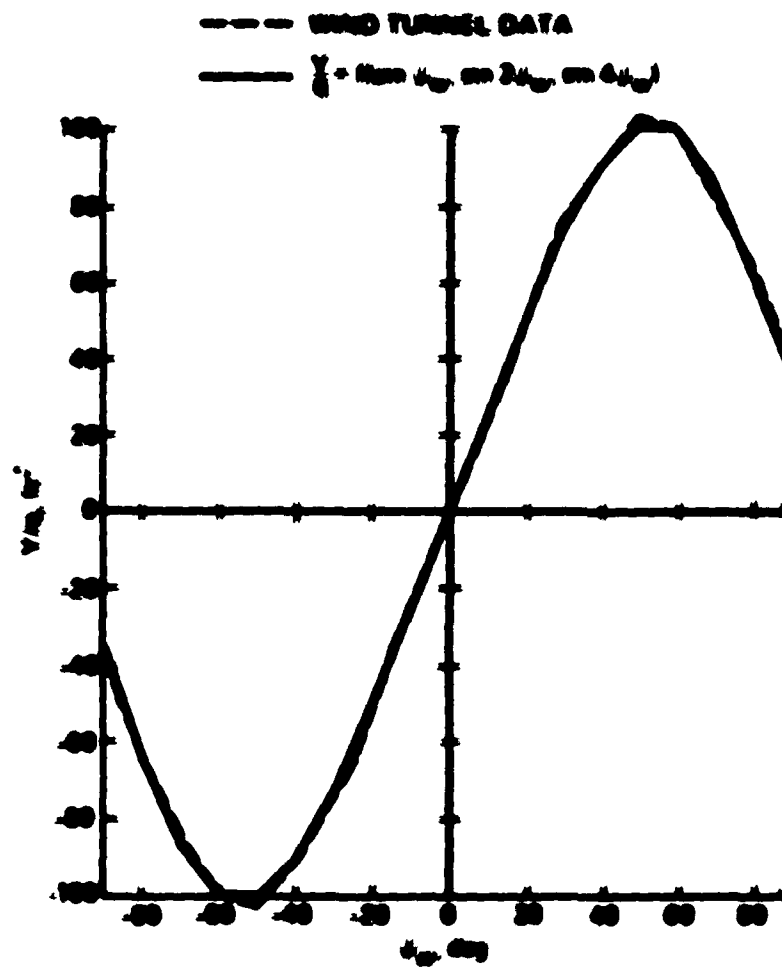


Figure 7.- Fuselage side force vs sideslip.

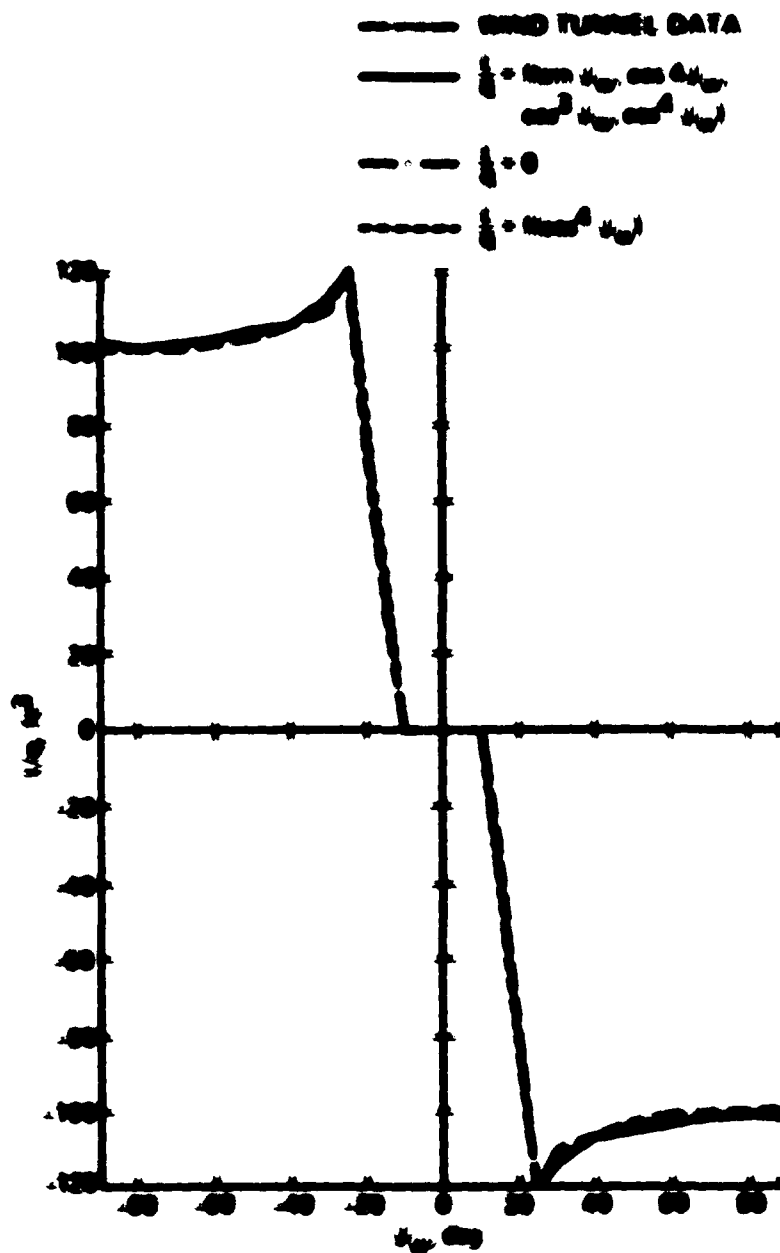


Figure 8.- Fuzelage rolling moment vs sideslip.

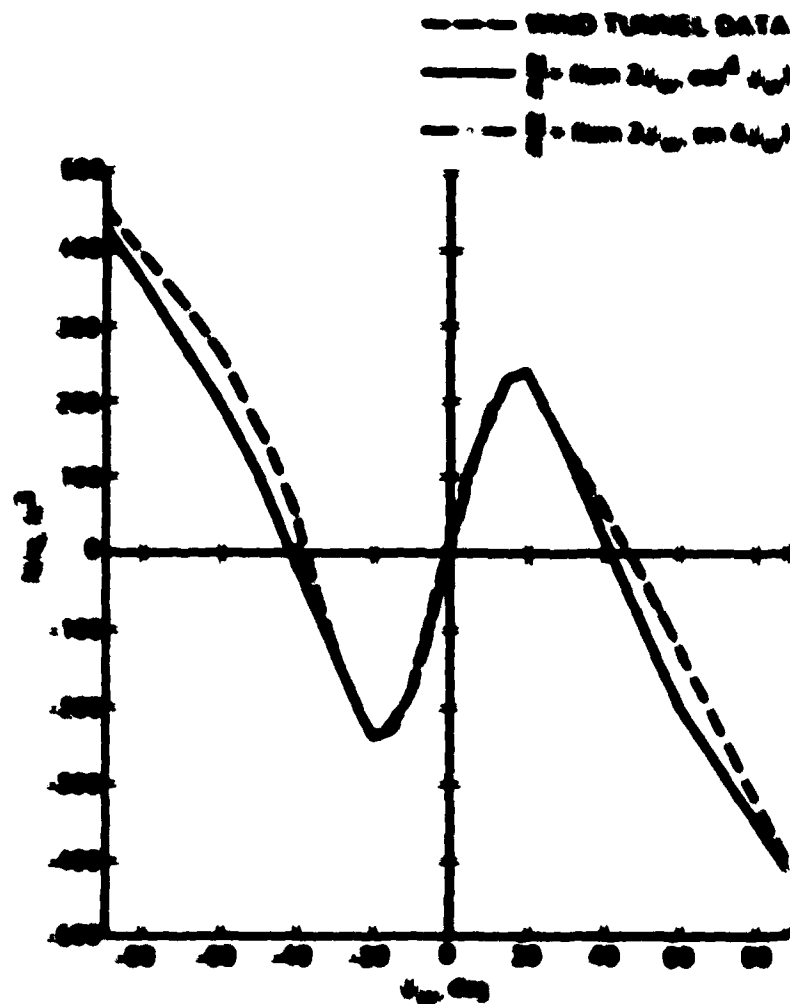


Figure 9.- Fuselage yawing moment vs sideslip.

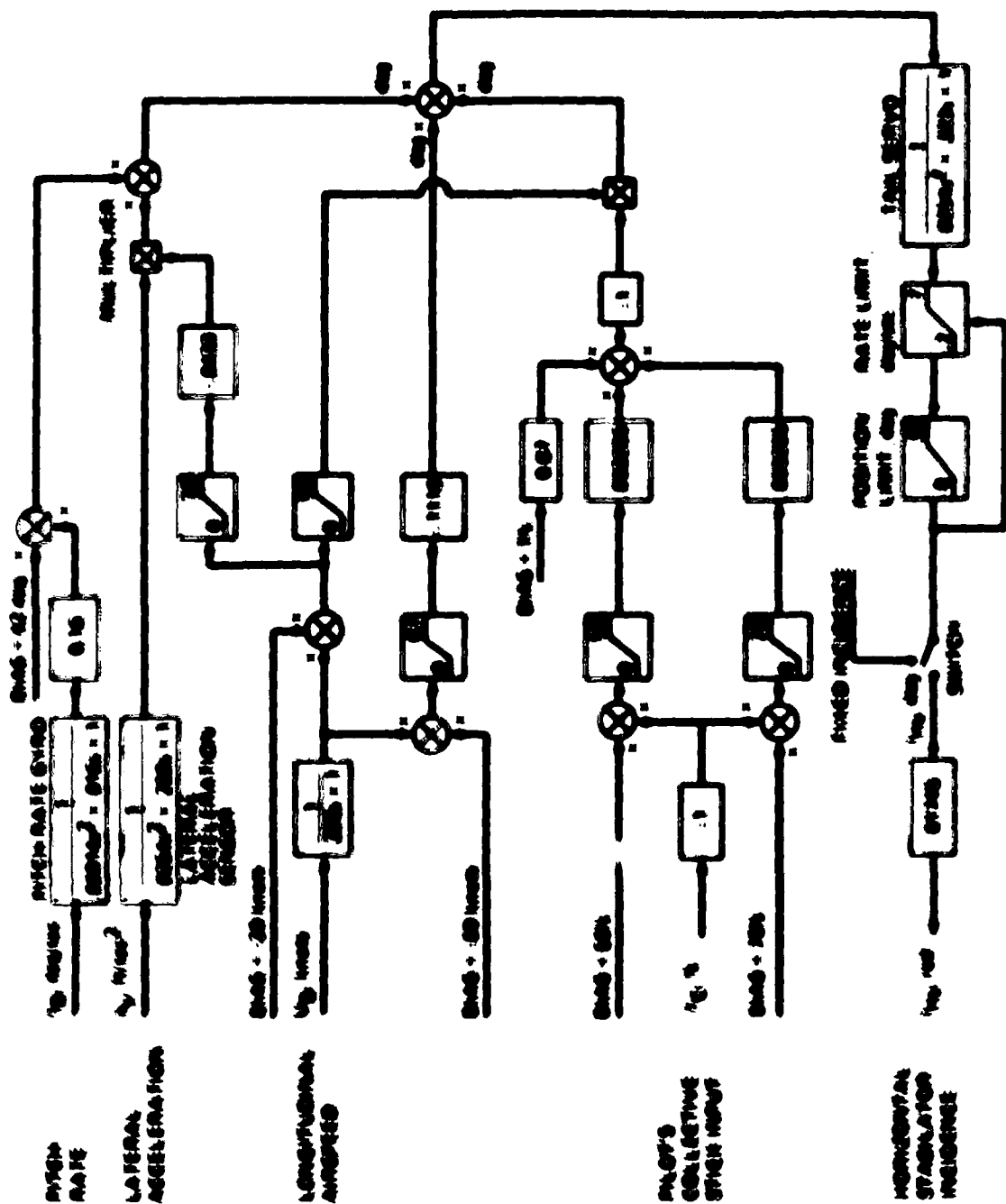


Figure 10 - H-60 horizontal stabilizer control system.

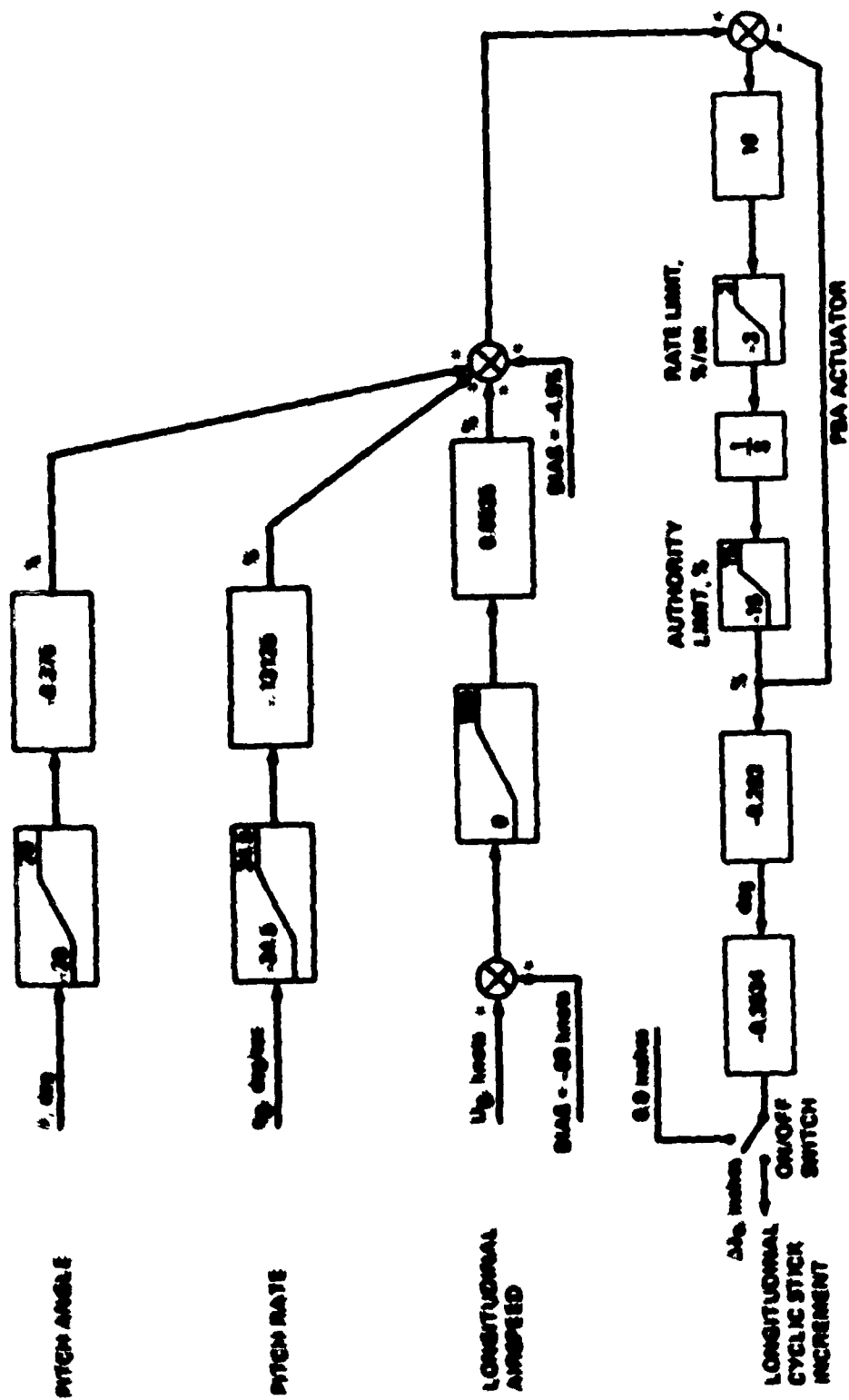


Figure 11.- UH-60 pitch bias actuator.

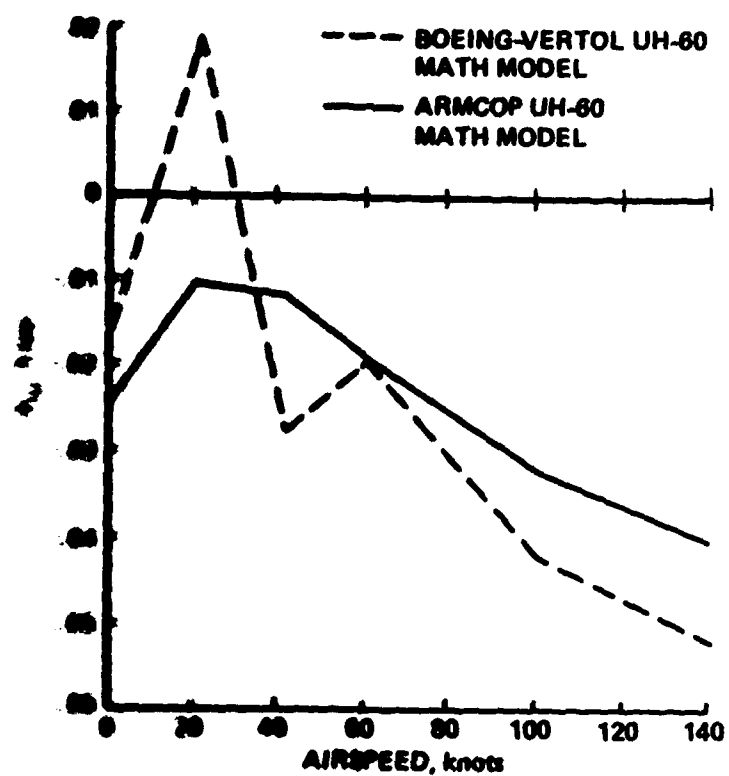


Figure 12.- Drag damping vs airspeed.

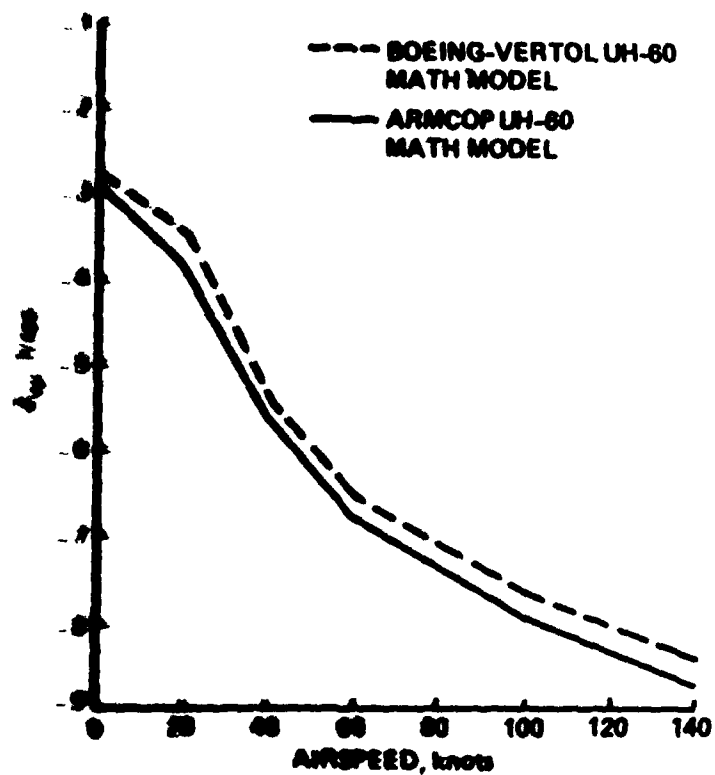


Figure 13.- Vertical damping vs airspeed.

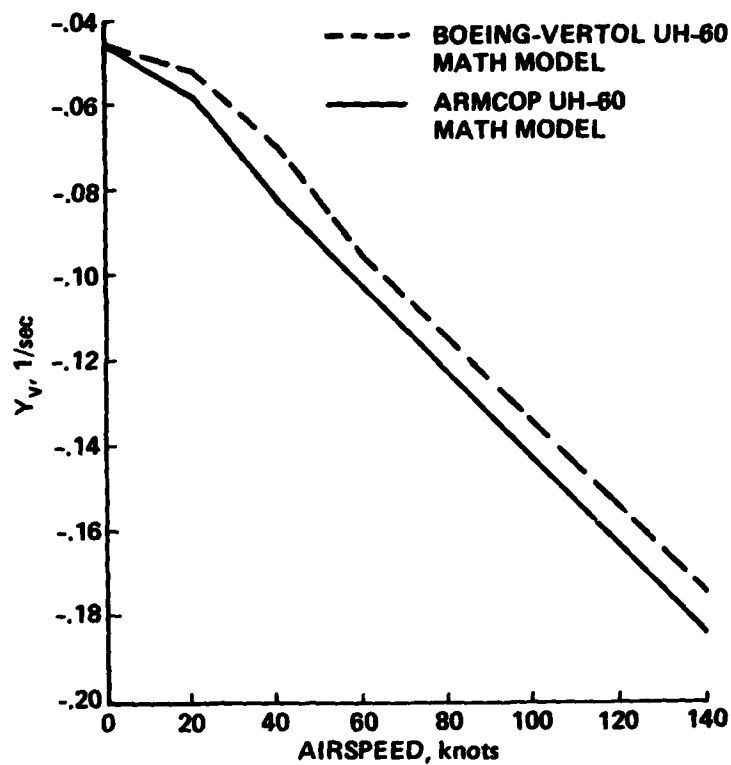


Figure 14.- Side-force damping vs airspeed.

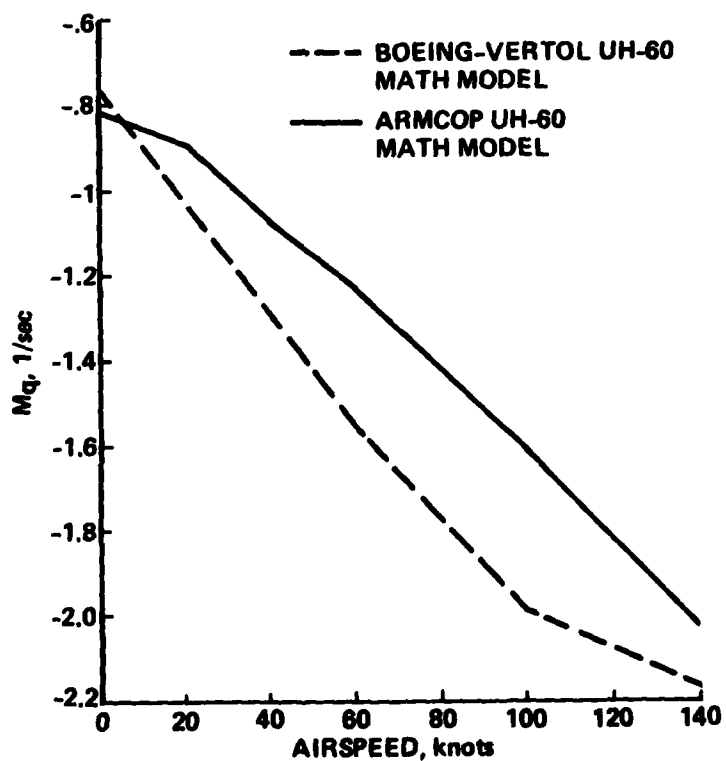


Figure 15.- Pitch damping vs airspeed.

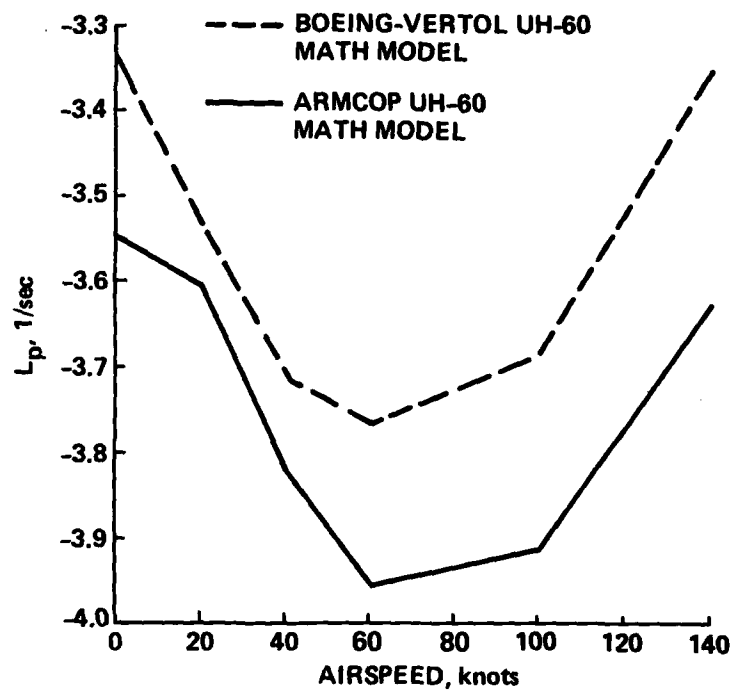


Figure 16.- Roll damping vs airspeed.

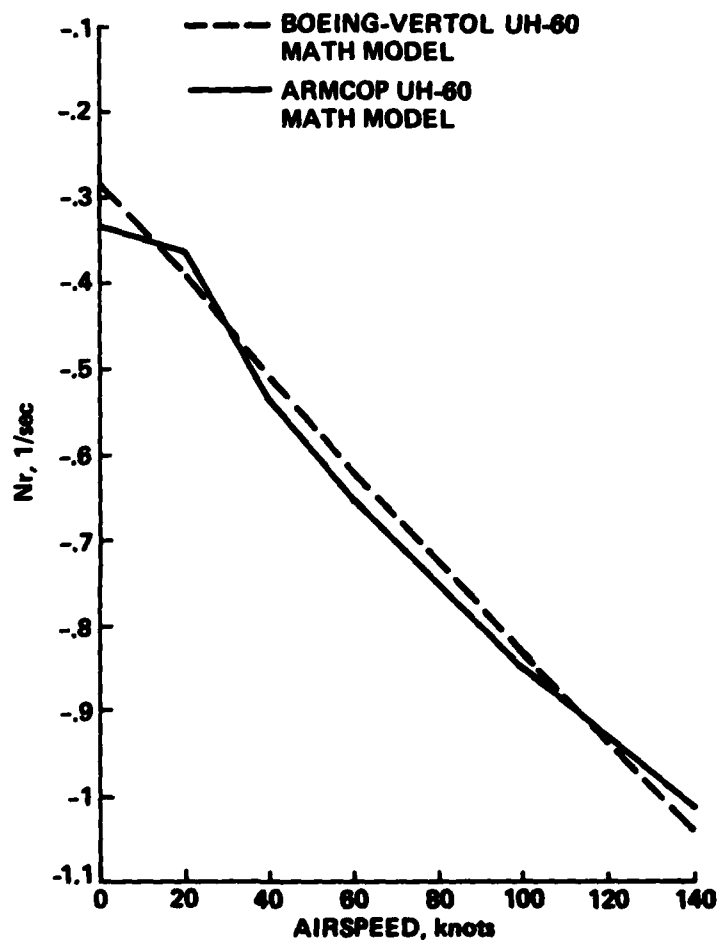


Figure 17.- Yaw damping vs airspeed.

1. Report No. NASA TM 85890 and USAAVSCOM TM-84-A-2		2. Government Accession No. AD- A145 899		3. Recipient's Catalog No.	
4. Title and Subtitle A MATHEMATICAL MODEL OF THE UH-60 HELICOPTER				5. Report Date April 1984	
				6. Performing Organization Code	
7. Author(s) Kathryn B. Hilbert				8. Performing Organization Report No. A-9646	
9. Performing Organization Name and Address Ames Research Center and Aeromechanics Laboratory, U. S. Army Research and Technology Laboratories -- AVSCOM, Ames Research Center, Moffett Field, CA. 94035				10. Work Unit No. T-6292	
				11. Contract or Grant No.	
12. Sponsoring Agency Name and Address National Aeronautics and Space Administration, Washington, D. C. 20546 and US Army Aviation Systems Command, St. Louis, MO. 63120				13. Type of Report and Period Covered Technical Memorandum	
				14. Sponsoring Agency Code 505-42-11	
15. Supplementary Notes Point of Contact: Kathryn B. Hilbert, MS 211-2, Moffett Field, CA. 94035 (415) 965-5272 or FTS 448-5272					
16. Abstract This report documents the revisions made to a ten-degree-of-freedom, full-flight envelope, generic helicopter mathematical model to represent the UH-60 helicopter accurately. The major modifications to the model include fuselage aerodynamic force and moment equations specific to the UH-60, a canted tail rotor, a horizontal stabilizer with variable incidence, and a pitch bias actuator (PBA). In addition, this report presents a full set of parameters and numerical values which describe the helicopter configuration and physical characteristics. Model validation was accomplished by comparison of trim and stability derivative data generated from the UH-60 math model with data generated from a similar total force and moment math model.					
17. Key Words (Suggested by Author(s)) Helicopter, Helicopter Aerodynamics, UH-60, Canted tail rotor, Horizontal stabilizer, Pitch bias actuator, Stability deriv- atives, Mathematical model, Simulator				18. Distribution Statement Unlimited Subject category 08	
19. Security Classif. (of this report) Unclassified		20. Security Classif. (of this page) Unclassified		21. No. of Pages 45	
				22. Price A03	